



International Conference on Computational Science, ICCS 2012

## Nanoscale analysis of plasticity and fracture of the sheet metal structures

A. Schmidt\*

*Department of Mechanical Engineering, Lipetsk State Technical University, Moskovskaya str. 30, Lipetsk, 398600, Russia*

---

### Abstract

The analysis at nano-scale is important for the modeling of plastic deformation and its structures. We reviewed algorithms at nano-scale using FEM and presented a solution for modeling of such processes and corresponding algorithms. Also, we studied dislocations and avalanches in the deformed body, how they affect the quality, and methods to decrease their affluence on the product. For meshing of the model proposed method is to relate particle size and mechanical properties, which is investigated in the context of plastic deformation. Damage models presented in the paper can be proved useful for the production modeling and manufacturing. Modeling of buckling and plastic deformation proved to be useful to study the phenomenon and can be optimized with the proposed methods. Numerical verification using test benchmarks were conducted to demonstrate flange buckling, its particle measurements, and avalanches in the deformed part to validate propositions.

Keywords: Nanoscale; plasticity; fracture; avalanches.

---

### 1. Overview

One of the basic observations of material science is the existence of a well-defined yield stress. We study by simulation, in three dimensions, plastic deformation of nano-scale objects under stress. In this contribution, we propose a method for alleviating problems with unknown factors affecting mesh for damage formulations. It makes it possible to construct predictable models employing CAD software for structural investigations and optimizations of the processes of plastic deformation. First, we review developed fracture model and developed model for isotropic damage formulation applied to the nano-scale domain space. Second, we study boundary value problem for particle interaction among part specimen using the implicit gradient model. Finally, we conduct test benchmarks to validate propositions and to show correctness of the proposed models.

---

\* Corresponding author. Tel.: +1-773-293-3115; fax:+1-773-213-9907  
E-mail address: [me@alexschmidt.net](mailto:me@alexschmidt.net)

### 1.1. Advantages of nanoscale analysis

There is a promise of computational science to decompose macroscopic complexity into microscopic simplicity for the domain specific problem resolution. The payoff is the increase for the high spatial and time resolution of the computational efforts. This is achieved via simplified problem formulation and removal of the empirical correcting coefficients, which leads to a clear understanding of the dependencies, and enhances understanding of the evolution at a much higher fidelity level.

### 1.2. Methodology

Let us consider a bulk material undergoing a plastic deformation, in which case various processes take place, including but not limited to dislocation and deformation of material particles, size and form changes, and emergence of defects. We study material processes at small specimen scale. Moreover, to study the behavior of the material we employed simulation using nano-scale equipment.

Because dislocations in the material are not uniform by definition, simulation should be performed for each block of material, but it's computationally extensive due to high interconnection factor between edges in network, which can be built to represent the material. Yield stress at small specimen size is not well-defined. Phenomenology of plastic deformation based on the statistical properties is not well-studied. It is observed that fluctuation of stress-strain is in response to damage of individual specimen. Irregular plastic response of submicron crystalline materials is conceived as a self-organizing phenomenon of strain avalanches. We present a statistical analysis of the fluctuating stress-strain response of individual chunks of metal. Main proposition is that fundamentally the stress-strain dependency holds the key to other empirical aspects of the flow [13]. We wanted to perform analysis of plastic deformation and emerging damage effects to further expand possible applications of such technique, which allows diminishing needs for corrective modifications of the details and accounting for potential defects in the metal.

## 2. Damage modeling

Furthermore, in this contribution we use isogeometric finite elements to model damage formulations. The analysis based on the isogeometric models was introduced by Hughes [14] and has been applied to a variety of problems. Their advantage includes relationship between geometry and solution space. To avoid mesh dependencies of the process we propose to relate the material properties to the element size. The proposed method is contained by mapping where an internal length scale can be introduced by a spatial smoothing function in the continuum formulation. Gradient approximations of this smoothing function have led to the development of damage models where an internal length scale is introduced through gradients of an equivalent strain field.

In this work, we study mechanisms of formation of dislocations and their parameters. To accomplish this, we're mapping macro model of plastic deformation to nano-scale particle. For the modeling, natural units should be introduced, such as velocity  $v$ , strain  $\gamma$ , stress  $\tau$  and dislocation density  $\rho$  to represent particle movements at specified scale. Let us consider potential modeling of fractures which can occur in the model based on the state of the part and each corresponding particle.

### 2.1. Fracture modeling

The damage models are used for continuum models to simulate physical defects arising in plastic deformation processes. The meshing of the model is proposed in an alternative way to adhere to the particle sizes. To avoid mesh dependencies we propose, based on the thoughts from [15], to relate material properties to the size of particle [16,17]. The model of gradient damage formulation, based on Taylor expansion is used to approximate to an integral, which derives from the two second-order PDEs and can be easily discretized because it is based on the  $C^0$ -continuous finite function.

### 2.2. Isotropic damage formulation

We consider a body  $\Omega \in \mathbb{R}^N$  with  $N \in \{1,2,3\}$  and boundary  $\partial\Omega$  where the displacement is denoted by  $u(x) \in \mathbb{R}^N$  for a material point  $x \in \Omega$ . Hence the assumption of the small displacement gradients resolved in form of infinitesimal strain tensor can be written as follows:

$$\varepsilon_{ij} = u_{(i,j)} = \frac{1}{2} \left( \frac{\partial u_i}{\partial x_j} + \frac{\partial u_j}{\partial x_i} \right) \tag{1}$$

The Cauchy stress tensor for the corresponding stress measure can be written as follows:

$$\sigma(x) \in \mathbb{R}^{N \times N} \tag{2}$$

An external traction  $\tilde{t}_i$  puts a pressure on the boundary  $\partial\Omega_{t_i} \subseteq \partial\Omega$  affects it and is calculated for tensor relationship between the Cauchy stress and infinitesimal strain tensor is expressed as:

$$\sigma_{ij} = (1 - \omega) H_{ijkl\epsilon kl} \tag{3}$$

where  $\omega \in [0,1]$  is scalar damage parameter,  $H$  – Hookean elasticity tensor for undamaged material ( $\omega = 0$ ). The material loses its stiffness when the following holds ( $\omega = 1$ ). The summary of the process for steps 1 to  $N$  results into  $u_i v_i = \sum_{i=1}^N u_i v_i$ .

The local damage law which describes the emergence of the defect appearance during a history of deformation ( $k$ ), which is expressed as  $\omega = \omega(k)$ . The history parameter  $k$  evolves according to the formula based on Kuhn-Tucker conditions:

$$f \leq 0, k \geq 0, kf = 0 \tag{4}$$

Non-local damage law is introduced by means of nonlocal equivalent strain  $\bar{\eta}(x)$  and the volume average of a local equivalent strain,  $\eta = \eta(\epsilon)$  as follows:

$$\bar{\eta}(x) = \frac{\int_{y \in \Omega} g(x, y) \eta(y) dy}{\int_{y \in \Omega} g(x, y) dy} \tag{5}$$

where  $g(x, y)$  is the weighting function calculated as:

$$g(x, y) = \exp\left(-\frac{\|x - y\|^2}{2l_c^2}\right) \tag{6}$$

This model is known as nonlocal damage formulation where the local equivalent strain maps to strain tensor via a scalar. While having major advantages, the disadvantage of this formulation from computational aspect is that it requires the computation of an integral for the evaluation of the constitutive behavior at every particle.

The nonlocal equivalent strain can be approximated via Taylor expansion as follows:

$$\eta(y) = \eta|_{y=x} + \frac{\partial \eta}{\partial y_i} \Big|_{y=x} (y_i - x_i) + \frac{1}{2} \frac{\partial^2 \eta}{\partial y_i \partial y_j} \Big|_{y=x} (y_i - x_i)(y_j - x_j) + > \mathcal{O}((x_i - y_i)^3) \tag{7}$$

Assuming the solid volume stretches to infinity leads to the gradient approximation of equation

$$\bar{\eta}(x) - \frac{1}{2} l_c^2 \frac{\partial^2 \bar{\eta}}{\partial x_i^2} (x) + \frac{1}{8} l_c^4 \frac{\partial^4 \bar{\eta}}{\partial x_i^2 \partial x_j^2} (x) - \frac{1}{48} l_c^6 \frac{\partial^6 \bar{\eta}}{\partial x_i^2 \partial x_j^2 \partial x_k^2} (x) + \dots = \eta(x) \tag{8}$$

The implicit gradient model that follows was adopted widely and is presented in detail below and used for defect modeling for the particles of the part.

### 2.3. Implicit gradient particle damage modeling

The implicit formulation required for the solution of a boundary value problem for a particle interaction. The nonlocal equivalent strain field,  $\bar{\eta}(x)$ , resulting boundary value problem for the third-order formulation, is evaluated using formula as follows:

$$\left\{ \begin{array}{l} \frac{\partial \sigma_{ij}}{\partial x_j} = 0 \quad \forall x \in \Omega \\ \mathcal{L}^d \bar{\eta} = \eta \\ \sigma_{ij} n_j = \tilde{t}_i \quad \forall x \in \partial \Omega_{t_i} \\ \frac{\partial}{\partial x_n} \left( \frac{\partial^\alpha \bar{\eta}}{\partial x_j \dots} \right) = 0 \quad \forall x \in \partial \Omega, \alpha \in \{0, \dots, n-2\} \\ u_i = \tilde{u}_i \quad \forall x \in \partial \Omega_{u_i} \end{array} \right. \tag{9}$$

where  $\tilde{t}$  is the predefined boundary traction and  $\tilde{u}$  is the displacement. The precondition is that boundary forces are equivalent for all directional derivatives, i.e.  $\frac{\partial}{\partial x_n} = \frac{n_i \partial}{\partial x_i}$ . To solve the equation using Galerkin method, the same solution spaces are used for the displacement field and nonlocal equivalent plastic strain field. Those are  $S_i^U \subset H^{\bar{z}}(\Omega)$  and  $S^{\bar{\eta}} \subset H^{\bar{z}}(\Omega)$  respectively. Then the weak form of (9) can be formulated as follows:

$$\left\{ \begin{array}{l} (\sigma_{ij}, v_{i,j}^u)_\Omega = (\tilde{t}_i, v_i^u)_{\partial \Omega} \quad \forall v_i^u \in V_i^U \\ (\bar{\eta} - \eta, v^{\bar{\eta}})_\Omega + \sum_{\alpha=1}^{d/2} (\mathcal{H}^\alpha \bar{\eta}, \mathcal{H}^\alpha v^{\bar{\eta}})_\Omega = 0 \quad \forall v^{\bar{\eta}} \in V^{\bar{\eta}} \end{array} \right. \tag{10}$$

To the discrete problem we applied Galerkin method [18], which formulated for the weak problem as follows:

$$\left\{ \begin{array}{l} (\sigma_{ij}, v_{i,j}^{u,h})_\Omega = (\tilde{t}_i, v_i^{u,h})_{\partial \Omega} \quad \forall v_i^{u,h} \in V_i^{u,h} \\ (\bar{\eta} - \eta, v^{\bar{\eta},h})_\Omega + \sum_{\alpha=1}^{d/2} (\mathcal{H}^\alpha \bar{\eta}, \mathcal{H}^\alpha v^{\bar{\eta},h})_\Omega = 0 \quad \forall v^{\bar{\eta},h} \in V^{\bar{\eta},h} \end{array} \right. \tag{11}$$

where  $\sigma_{ij}$  – carchy stress tensor and  $\sigma_{ij} \in V$ ;

$V$  –a Hilbert space;

$\bar{\eta}$  –norm of nodes;

$\Omega$  –problem space;

$v_{i,j}^{u,h}$ –weighting function.

Using the function of NURBS as trial function  $\{R_i(x)\}$ , the former results in a system  $(N + 1)n$  as follows:

$$\begin{cases} f_{int,k}^{u_m} = f_{ext,k}^{u_m} & \forall (k, m) \in \{1 \dots n\} \otimes \{1 \dots N\} \\ f_{int,k}^{\bar{\eta}} = 0 & \forall k \in \{1 \dots n\} \end{cases} \quad (12)$$

For the damage formulation for third-order problem, where  $n = 3$ , the linear operator  $\mathcal{H}^\alpha$  is written as follows

$$\mathcal{H}^3 = \frac{l_c^3}{\sqrt{48}} \frac{\partial^3}{\partial x_i \partial x_j \partial x_k} \quad (13)$$

Hence, for the six-order formulation using (13) damage model can be calculated using the following formula:

$$\sum_{\alpha=1}^{\frac{d}{2}} = \int_{\Omega} \frac{l_c^2}{2} \frac{\partial \bar{\eta}}{\partial x_i} \frac{\partial v^{\bar{\eta}}}{\partial x_i} + \frac{l_c^4}{8} \frac{\partial^2 \bar{\eta}}{\partial x_i \partial x_j} \frac{\partial^2 v^{\bar{\eta}}}{\partial x_i \partial x_j} + \frac{l_c^6}{48} \frac{\partial^3 \bar{\eta}}{\partial x_i \partial x_j \partial x_k} \frac{\partial^3 v^{\bar{\eta}}}{\partial x_i \partial x_j \partial x_k} d\Omega \quad (14)$$

where corresponding fourth and six-order results can be extracted by ignoring the third and second-order spatial derivatives in the (14) above. To validate the developed method, the nano-deformation experiments have been conducted on an indenter. We applied developed method to the benchmark problems and evaluated principal metrics. Tests modes also included measurement of the flange buckling and grain measurement. To conduct multistep optimization process, principles outlined in [7] were applied.

### 3. Benchmarks

#### 3.1. Numerical verifications

The typical problem with parts formed using drawing is the buckling of the flange, which usually means the specimen is defective and micro-level voids are emerging near the deformation into buckling. Modeling of this phenomenon is done using steel sheet designed to undergone the stress test where stress is exceeding plasticity.

The simulations to verify the described propositions were performed for the testing problems. We consider a model loaded in extraction as shown in Fig. 1. The 40 mm deep drawing was conducted on the model using tool with profile decreased. For each step, the characteristic values were calculated [13].

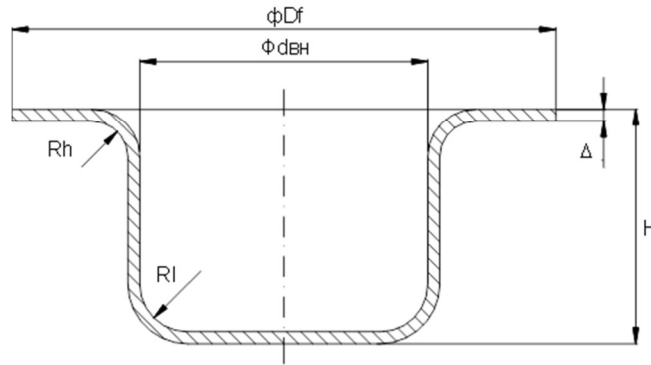


Fig. 1. Schematic representation of a three-dimensional model loaded under pressure.

The problem was formulated using Galerkin method for different number of elements, see Table 1 below.

Table 1 Problem size and results

Number of elements $m$	80	160	320	800	1600
Number of nodes, $n$	90	170	340	880	1800
Number of discontinuities	17	29	14	17	4

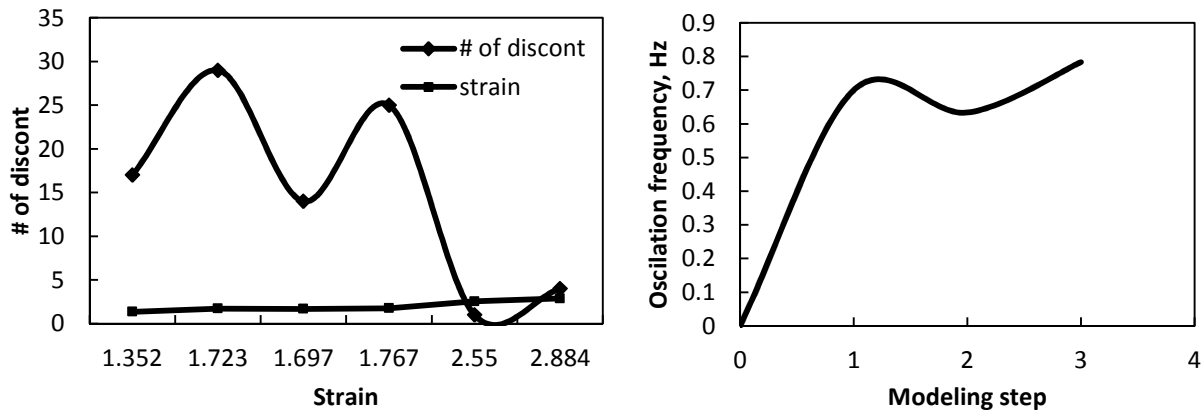


Fig. 2. Oscillation of elements and number of discontinuities

The finite element solution tends to oscillate with some frequency when pressure is applied and discontinuities to appear, unless the solution is stabilized, see Fig. 2. Disadvantage of the stabilized solution is causing numerical dissipation, which decreases the accuracy [19]. To overcome this, we use spacetime-discontinuous Galerkin method, proposed in [20]. This method has lower probability for oscillation so that direct patch-by-patch advancing front is generated with linear computational complexity (cf. sec. 3.1, [19]).

The results obtained during simulation suggest that only long-range interactions between dislocations are captured for the submicron level of plastic flow.

### 3.2. Test 2: Numerical verifications of avalanches

Stress-strain dependency can be derived for this model. It can also be observed that the avalanches are present in the model during the plastic flow simulation. Avalanche state can be derived as a norm of stress, i.e.

$$\|P\| = \sum_{i=1}^m |x_i| \tag{15}$$

The simulations of plastic strain response measured to determine patterns of avalanche development during plastic deformation.

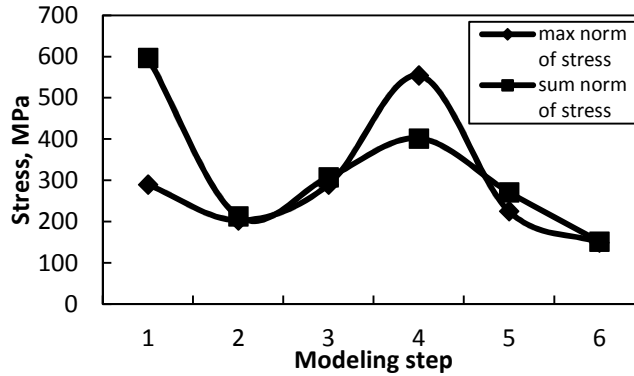


Fig. 3. Model in avalanche state

We've built the graph of the dependencies between the modeling step and norm of the stress for the model in avalanche state, see Fig. 3. Measurements were obtained for stress vs. plastic strain dependency and indicate strain avalanches stochastic propagation for different samples, which converges into dominating front.

Furthermore, tail of avalanche velocity distribution comes from the system in avalanche state. The goal here is to minimize the effect of avalanches into form of the part, which improves quality of the product.

In conclusion the correlation produces finite amplitude [17]. Then stress and velocity distribution must have reciprocal dependency.

### 3.3. Test 3: Grain measurements of buckled particles

The resulting material state was captured and the size of the grains was obtained using transmission electron microscope. We study the elastic-plastic behavior of the metal with the emphasis on the effects of microstructure.

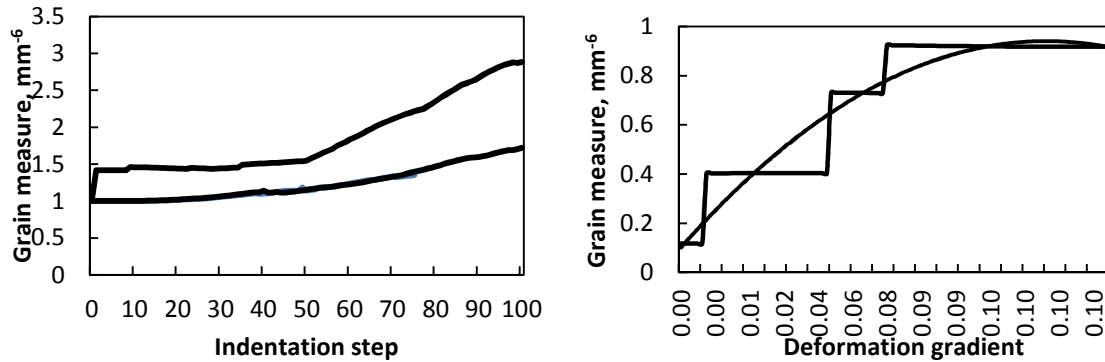


Fig. 4. Grain measurement

The force-displacement curves were obtained using the meshes. It is observed that with increased order of magnitude, the approximation of the result improved, Fig. 4.

We can conclude that for submicron sizes the dependency between stress and strain holds and it is represented as smooth function with the representative points specific to a particular material. The theoretical similarity between strain response curves suggests that general behavior is captured for the nano-scale particle flow.

## 4. Discussion

### 4.1. Dynamics of dislocations

It is rather difficult to measure deformations and hence dislocations directly in the modeled problem. The availability of the results is scarce and we performed modeled dislocation measurement from the experiment simulation. The strains were measured during the individual stress-controlled simulations. The results indicate presence of strain avalanches, which result in different deformation patterns for difference sample experiments. In the observation it was determined that there are many definitions for deformation and for strain. It is hard to introduce infinitely many versions and it's difficult to determine one which constitutes an elastic relation. Natural assumptions can be made regarding correlation of dislocations. Previously [21] it was shown that stresses in the internal locations are distributed stochastically.

### 4.2. Correlation between nanostructures and mechanical behavior

It was observed that mechanical behavior observed through cold drawing confirms hypothesis when larger scale deformation can be projected to the nano-level deformation. Quasi-static stress-strain curves are retained for the strain of the grains, which conforms to our model and results for plastic deformations.

### 4.3. Nanostructures and their evolution

Traditional discreet approximations cannot capture localized deformation areas on the order of nanoscale characteristic lengths. Constitutive behavior at these significantly smaller scales is usually cannot be projected into macroscale average behavior. The important material behavior is difficult to explain including fracture and strength using conventional methods, but can be elaborated more clearly using proposed method.

Presence of strain hardening can be explained through anisotropic properties of the modeled material. Dislocation pileup at grain boundaries is present near the areas affected by buckling.

Non-uniform dislocation distribution between regions near grain boundary and the grain interior is emerging due to the non-uniform deformation between regions. We've employed the continuum theory which fully describes material using matrix representation and process parameters. The  $(\mathcal{H}^\alpha, \bar{\eta}(x), v_{i,j})$  describes inhomogeneity in the matrix. The damage models are used for continuum models to simulate the physical defects arising in plastic drawing processes were found applicable to the problem domain.

## Conclusion

The nano-deformation has been examined in the context of plastic deformations. Assumed stress-strain formulation was extended to nano-scale and tested in large deformation and problems typically solved by finite elements. We adopted isogeometric projective formulation is response for the volumetric damage, without resort to other techniques. The presented simulations show high predictability for characteristics formulated in other well-known methods.

## References

- 1 Huang Y, Zhang F, Hwang KC, Nix WD, Pharr GM, Feng G. A model of size effects in nano-indentation. *Journal of the Mechanics and Physics of Solids*. 2006;54:1668–1686.
- 2 Hedayatia A, Najafzadeha A, Kermanpur A, Forouzana F. The effect of cold rolling regime on microstructure and mechanical properties of AISI 304L stainless steel. *Journal of Materials Processing Technology*. 2010;210(8):1017-1022.
- 3 Chena H, Li L, Yua W. Multiscale finite element analysis of bulk nano-particle fabrication by a mechanical method. *Journal of Materials Processing Technology*. 2009;209(9):4243-4247.
- 4 Farsad M, Vernerey FJ, Park HS. An extended finite element/level set method to study surface effects on the mechanical behavior and properties of nanomaterials. *INTERNATIONAL JOURNAL FOR NUMERICAL METHODS IN ENGINEERING*. 2010;84:1466–1489.
- 5 Yvonnet J, Le Quang H, He QC. An XFEM/level set approach to modelling surface/interface. *Comput Mech*. 2008;42:119–131.
- 6 Slebodaa T, Muszkaa K, J. M, Haleb P, R.N. W. The possibilities of mechanical property control in fine grained structures. *Journal of Materials Processing Technology*. 2006;177(1-3):461-464.
- 7 Sanaty-Zadeh A. Comparison between current models for the strength of particulate-reinforced metal matrix nanocomposites with emphasis on consideration of Hall–Petch effect. *Materials Science and Engineering*. 2011.
- 8 She H, Wang B. A geometrically nonlinear finite element model of nanomaterials with consideration of surface. *Finite Elements in Analysis and Design*. 2009;45:463–467.
- 9 Parashar SKS, Padhi P, Awalendra K, Thakur RNP. Finite Element Model in Nanoindentation to Study Nonlinear Behavior of Nanoceramic PGZT. *Materials and Manufacturing Processes*. 2007;22(3):337-340.
- 10 Zonga Z, Loua J, Adewoyeb O, Elmustafac A, Hammadd F, Soboyejoa WO. Indentation Size Effects in the Nano and Microhardness of FCC Single Crystal Metals. *Materials and Manufacturing Processes*. 2007;22(2):228-237.
- 11 Zhang F, Huang Y, Hwang K, Qu CS, Liu C. A Three-Dimensional Strain Gradient Plasticity Analysis of Particle Size Effect in Composite Materials. *Materials and Manufacturing Processes*. 2007 ;22(2):140-148.
- 12 Hurang H, Onyebuekea L, Abatanb A. Characterizing and Modeling Mechanical Properties of Nanocomposites- Review and Evaluation. *Journal of Minerals & Materials Characterization & Engineering*. 2010;9(4):275-319.
- 13 Schmidt AA. Parallel multi-constrained partitioning schemes applied to the problems of deep drawing processes of sheet metal. In: *Proceedings of ICCES'10*; 2010; Las Vegas, NV. p. 365-377.
- 14 Hughes TJR, Cottrell JA, Bazilevs Y. Isogeometric analysis: CAD, finite elements, NURBS, exact geometry, and mesh refinement. *Computer Methods in Applied Mechanics and Engineering*. 2005;194:4135–4195.
- 15 Verhoosel CV. An isogeometric analysis approach to gradient damage models. *The Institute for Computational Engineering and Sciences, The University of Texas at Austin*; 2010.
- 16 Williams KJ, Bicanic N, Sture S. Constitutive and computational aspects of strain-softening and localization in solids. New York: ASME; 1984.
- 17 Cooley JW, Tukey JW. An algorithm for the machine calculation of complex Fourier series. *Math. Comput*. 1965;19:297–301.

- 18 Schmidt AA. Numerical Prediction And Sequential Process Optimization In Sheet Forming Based On Genetic Algorithm. *Materials and Manufacturing Processes*. 2011;26:521–526.
- 19 Abedi R, Haber RB, Thite S, Erickson J. An h–adaptive Spacetime–Discontinuous Galerkin Method for Linearized Elastodynamics. *à Revue européenne des éléments finis*, le. 2005.
- 20 Richter GR. An explicit finite element method for the wave equation. *Applied Numerical Mathematics*. 1994;16(1-2):65-80.
- 21 Stankovic L, Mosler J. Numerical Prediction of Macroscopic Material Failure. *Proc. Appl. Math. Mech*. 2006;6:197–198.
- 22 Brekelmans WAM, de Vree JHP. Reduction of mesh sensitivity in continuum damage mechanics. *Acta Mechanica*. 1995;110(1-4):49-56.